

On the discovery of Quasi-Periodic Oscillations in the polar CTCV J1928–5001

Hannes Breytenbach^{*1,2}, Dr. David Buckley², and Prof. Patrick Woudt¹

¹*University of Cape Town* ²*South African Astronomical Observatory*

January 9, 2023

Abstract

We report the results from a high speed photometric campaign on the recently discovered eclipsing mCV, CTCV J1928–5001, a.k.a. V379 Tel. We obtain unfiltered high time resolution (0.1 s to 1 s) photometry on the source for a total of 13 nights with the SAAO 1.9-m, and 1.0-m telescopes, utilizing the Sutherland High-Speed Optical Camera (SHOC) EM-CCD cameras and the HIgh Speed Photo-Polarimeter (HIPPO) instrument, as well as with SALT using the SALTICAM instrument. The source displays strong flickering and a deep eclipse. A frequency spectrum analysis revealed the presence of a faint QPO in the optical light of J1928-50. Fast QPOs in mCVs are very rare, with this discovery marking only the 6th source to display this phenomenon, and the first new such detection in over two decades. The QPO is centred on a median frequency of 0.35 Hz, and has power spread across a bandwidth of 0.3 Hz. Dynamic power spectra of the light curves shows that the QPO is only present during both bright phases of the orbit, and not during the eclipse. Our data samples the orbital light curve at unprecedented phase resolution, resolving both the eclipse ingress and egress, allowing us to refine the orbital period measurement to $(6\,061.8 \pm 0.1)$ s.

The Polar CTCV J1928–5001

J1928-50 was discovered by [Tappert et al. \(2004\)](#) in a follow-up campaign of colour selected candidate CVs from the Calán-Tololo Survey ([Maza et al., 1989](#)). Spectroscopy revealed the presence of multiple stellar components, including signatures of an M5V secondary in the red part of the spectrum, as well as Balmer absorption lines from the photosphere of the WD primary. The system was found to be an eclipsing source, with an orbital period of ~ 101 min. [Tappert et al. \(2004\)](#) measured an average out of eclipse V-band magnitude 17.85 ± 0.15 from observations conducted in 1996, while estimating the mid-eclipse magnitude as 21.05 ± 0.30 . Photopolarimetric observations from [Potter et al. \(2005\)](#) confirmed J1928-50 as a magnetic CV. During these latter observations, the source appeared somewhat brighter than previously seen, with an estimated V-band magnitude of ~ 16 – 17 measured from observations conducted in August 2003 (although no flux calibration was done in that study). Individual eclipse light curves occasionally resolved into 7 different components, namely the stream ingress, a pre-eclipse plateau, the primary ingress, total eclipse, primary egress, post-eclipse plateau and stream egress. Polarimetry revealed the presence of two accretion spots separated by $\leq 180^\circ$ in phase on the WD surface. This is indicated by the reversal in orientation of the circular polarization across the orbit, caused by cyclotron emission from accretion regions with opposite magnetic polarity. The circular polarization contribution varies between -8% to 12% in the red and between 0% to 5% in the blue parts of the spectrum respectively. [Potter et al. \(2005\)](#) estimates the magnetic field in J1928-50 to be ~ 20 MG.

* hannes@sao.ac.za

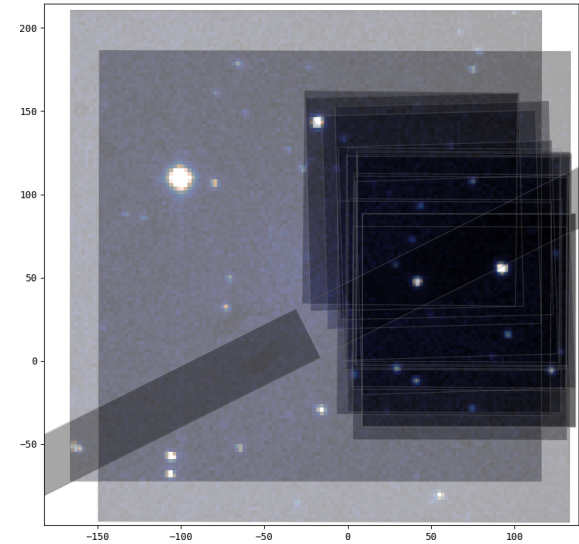


Figure 1: Mosaic of nightly snapshot images from SHOC on the SAAO 1.0m (wider field images) and 1.9m telescopes, as well as from SALT with SALTICAM (diagonal image strip).

Archival Observations

The Gaia parallax distance to J1928-50 is (130.7469 ± 0.0012) pc, making it the 8th closest mCV. J1928-50 also appears in the Swift X-Ray Telescope Point Source Catalogue (2SXPS, Evans et al. (2019)) with a count rate of (0.264 ± 0.067) counts/s in the 0.3 keV to 10 keV range, and a hardness ratio (HR1) of 0.203. The Million Optical Radio/X-Ray Associations (MORX, Fleisch (2016)) catalogue indicates an association between optical and X-ray with confidence of 65.3%.

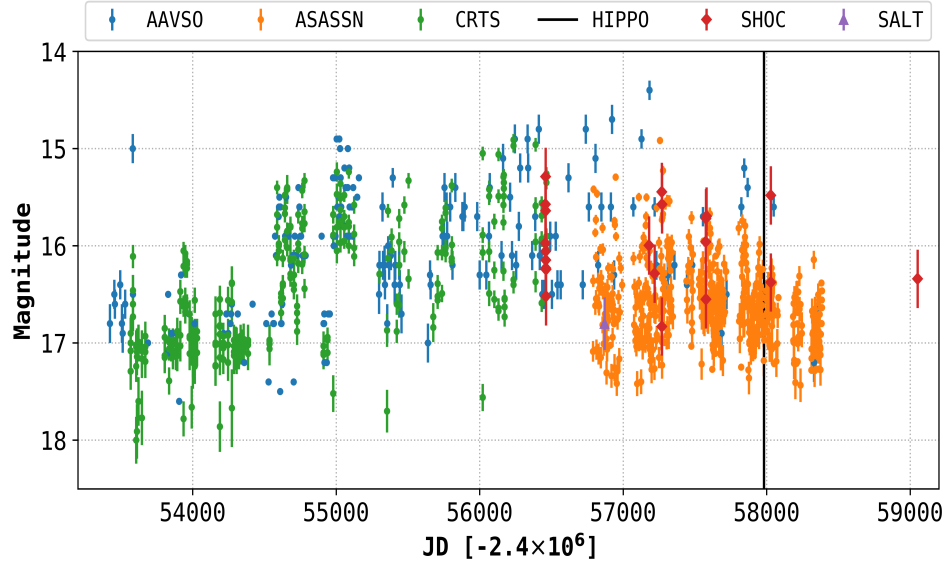


Figure 2: Long term light curve of J1928-50. Supplementary data from AAVSO, CRTS and ASASSN. Mean magnitudes of from SHOC and SALTICAM observations are also included

The Catalina Real-Time Transient Survey (CRTS, Drake et al. (2014)) has photometry of J1928-50 covering just under 8 years, while AAVSO International Variable Star Index (VSX, Watson et al. (2006)) (Watson et al., 2006, (Version 2020-05-18)) observations span ~ 13.5 years. The sparsity of data from these two surveys in latter years is admirably complemented by data from All-Sky Automated Survey for Supernovae (ASASSN, Jayasinghe et al. (2019)), spanning ~ 4.5 years between May 2014 and Oct 2018. These data are plotted in Figure 2, along with the observations conducted during our campaign on J1928-50. The V-band magnitude of the source varies between 14.5 to 18. There is some evidence of multiple accretion states in this long term light curve. This is indicated by a stepped feature at $\text{MJD} \approx 54600$ (April 2008) at which time the source seems to have gained in brightness by 1.5 magnitudes. The scatter in the data remains large across the entire time span of the observations and is consistent between CRTS and AAVSO data, indicating large intrinsic variations in the source brightness. This scatter seems to have increased with the brightening of the source which is consistent with the known rms-flux relation in compact accretors (Scaringi et al., 2012). There are also a number of points that are marked outliers on the faint end of the magnitude distribution. Using the ephemeris from Potter et al. (2005), we show that at least some of these faint points correspond to observations taken during an eclipse. These are marked by green circles in Figure 2. Curiously, some of the brightest observed points in this light curve are also near-eclipse. These are most likely due to exposures that partially overlap with the eclipse, but mostly cover the brightest phases of the orbit that precede and follow totality.

SAAO Photometry

J1928-50 was observed at the SAAO Sutherland site as part of a campaign aimed at characterising the high time resolution variability of known QPO sources as well as to search for new QPO sources among Polars. J1928-50 was targeted as an appropriate candidate since it is relatively bright, having a V magnitude of 16 d to 18 depending on the state, and a southern latitude, allowing for long-duration, short-exposure observations. Initial photometric observations for this campaign were conducted in 2013 using SHOC in EM mode at 0.1 s exposures during dark moon conditions. The exposure time was chosen to be as short as possible in order to sample the rapid variability of the source, while still maintaining an snr high enough to detect the presence of faint variability, typically on the order of a few percent of the source brightness. Analysis of the initial observations see section revealed the presence of a faint QPO in the unfiltered light curve of J1928-50 and motivated follow up observations with SALT using SALTICAM, as well as continued observations with the 1.0-m and 1.9-m SAAO telescopes. All counted, light curves spanning 40^m to 3.5^h in duration, were obtained on across 15 different nights over the course of 51 months. These fully resolve the entire orbit of J1928-50 including the eclipse ingress and egress at unprecedented phase resolution.

Light curve characteristics

Figure 3 shows the full set of differential light curves obtained during our campaign on J1928-50. All light curves, save that from SALT, cover the eclipse beginning at phase 0, and extending to phase 0.29. The overall shape of the eclipse appears similar to that described by Potter et al. (2005). The level of flickering, however, is much greater than that observed in 2003, and we therefore do not resolve the detailed substructure seen at that time. One orbital cycle contains two bright phases that have similar brightness and levels of flickering. Even though the source appears brighter in the 2013 data than previously seen, and the level of flickering has increased, the overall morphology of the orbital cycle remains largely unchanged. Particularly, the position of the eclipse within the bright phase has not changed, implying an unchanged accretion geometry despite the increased mass transfer rate.

Orbital Period

The eclipse ephemeris from Potter et al., 2005 is still accurate to within 1 s. The higher time resolution of our dataset, allows us to improve the accuracy of the ephemeris. We follow an identical procedure to Potter et al., 2005: Both the eclipse ingress and egress, which we completely resolve, provide precise fiducial markers for the basis of the ephemeris. Mid eclipse times are computed by averaging the mid ingress and egress times. Combining our data of the measured eclipse timings with that from previous studies, we present a modest refinement of eclipse mid-ingress ephemeris.

$$HJD = 2452879.2813386(58) + 0.070162312(9)E \quad (1)$$

Frequency Spectrum analysis and detection of a QPO

The high speed SHOC photometry from 2013 and SALTICAM in 2014 enables us to investigate the rapid variability of J1928-50 through spectral estimation techniques. Our primary analysis of the SHOC data utilizes the FFT, since the data are evenly sampled. For the SALTICAM data, using an FFT is not appropriate since the light curve contains periodic gaps due to the way in which data is read out from the CCD in frame transfer mode. We therefore employ the Lomb-Scargle Periodogram (LSP) to assess the frequency content of the SALTICAM light curve.

According to Potter et al. (2005), J1928-50 is accreting on two poles. To aid our understanding of the generative mechanism producing QPOs, it would be beneficial to know if QPOs are produced at one, or both poles on J1928-50. In the case of an offset dipole magnetic field, we expect different field strengths at the two accreting poles, and therefore expect different properties in the accretion zones and post-shock regions. In order to investigate such potential differences, we compute the sequence of phased average periodograms spanning the orbit. We split the light curves into 20 phase bins, compute the individual periodograms for each light curve segment and median combine the results across all light curves. The resulting phased

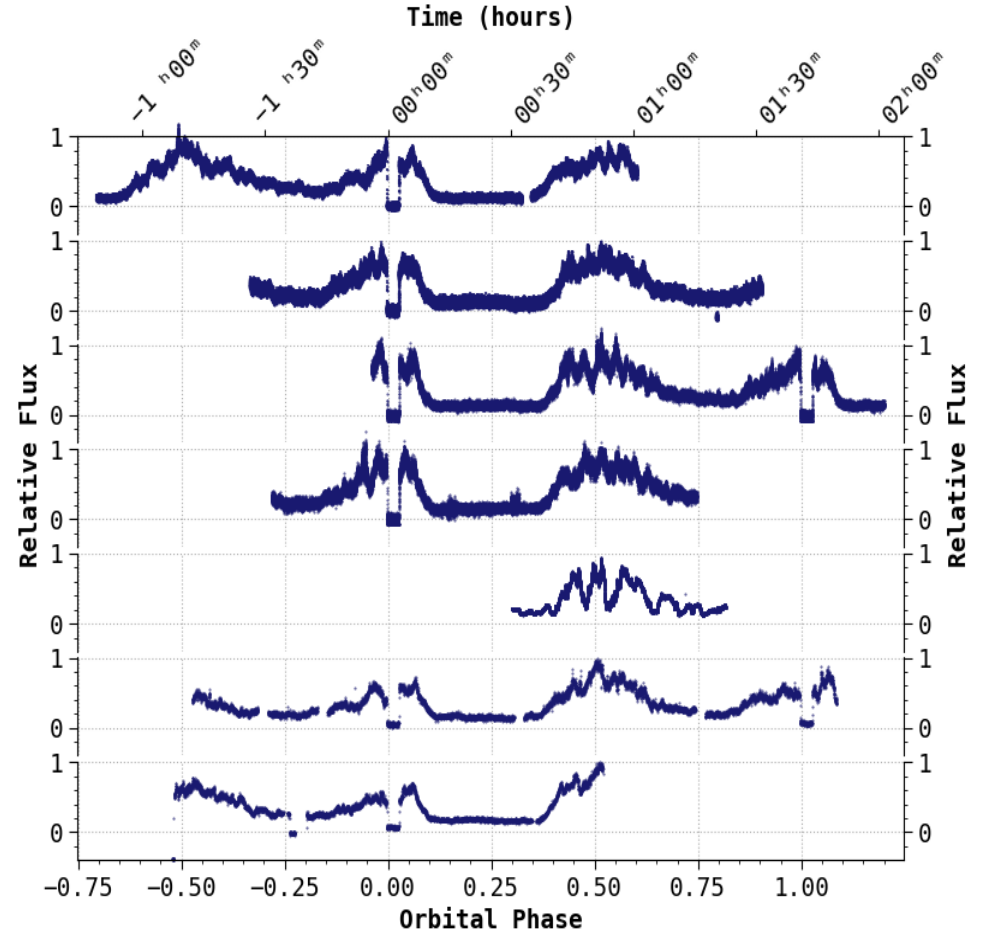


Figure 3: Individual nightly light curves for J1928-50 in chronological order from top to bottom. All light curves are unfiltered (or clear filtered in the case of SALT). Each light curve is displayed on the same scale in units of relative flux of the comparison star. The lower horizontal axis is given in units of the orbital period using the ephemeris in Equation 1, while the upper- gives the relative time from eclipse mid-ingress.

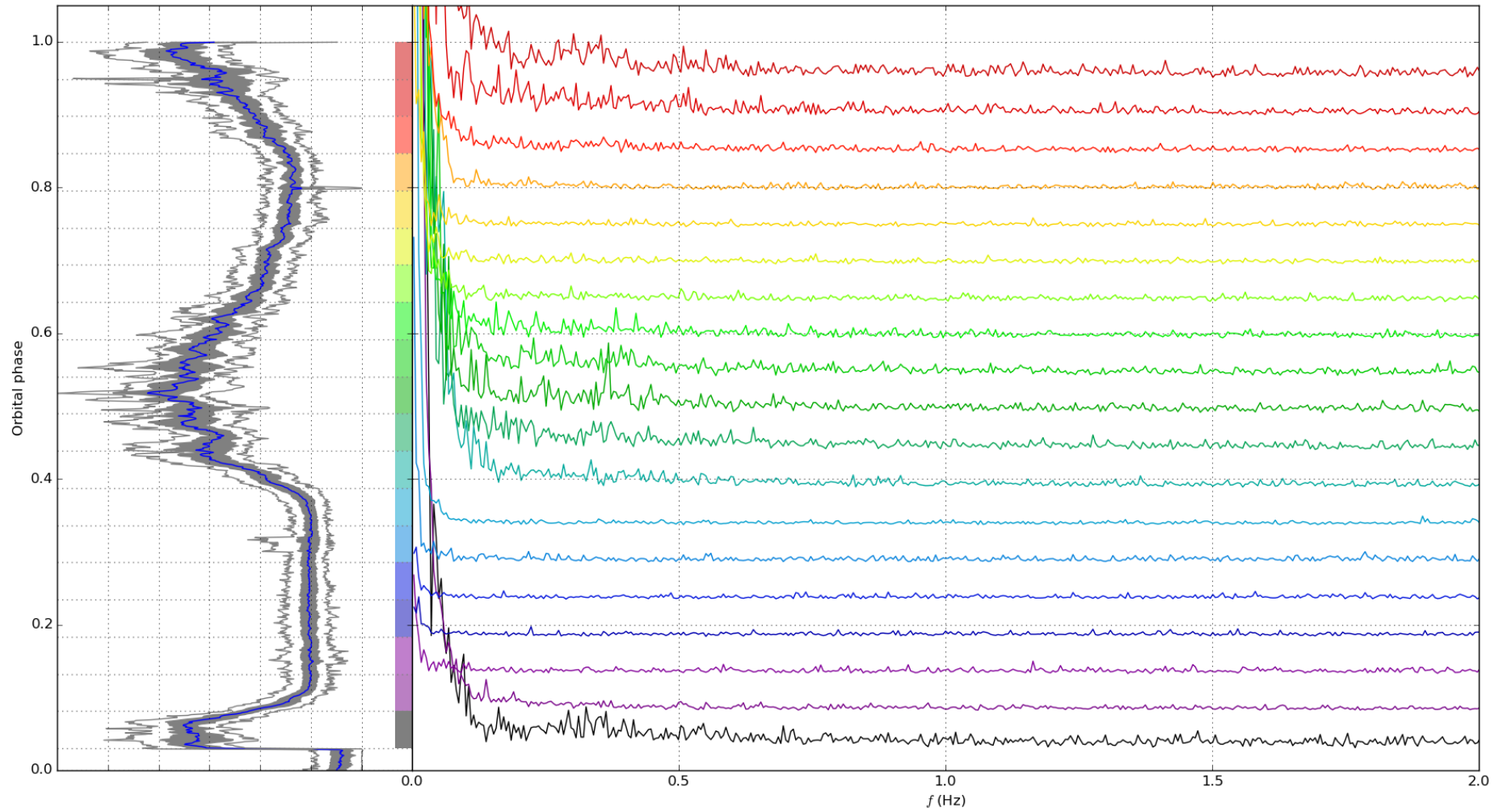


Figure 4: Phase resolved periodograms for J1928-50. **Left panel:** The average phase folded light curve with orbital phase plotted on the vertical axis and flux plotted on the horizontal axis. **Right panel:** Average phase resolved periodograms for combined light curve data. Each periodogram is coloured for the phase window it represents with corresponding bin sizes indicated in a colour sequence on the left side of this panel. The signature of the QPO can be seen as an increased power level at frequencies in the range 0.2 Hz to 0.5 Hz. The periodogram covering the eclipse phase is not shown.

average periodograms are shown in Figure 4. This shows that the QPO is strongest at phases immediately preceding- and following the eclipse. This represents the angles for which our view onto the primary accretion zone is most direct.

Discussion

High frequency QPOs of the kind detected here in J1928-50 are generally understood to be generated by shock-driven oscillations in the accretion column on the WD surface. As infalling material from the donor star reaches the WD, a transition from a relatively cool, supersonic flow to a extremely hot subsonic flow occurs via a strong hydrodynamic shock through which infalling material sharply decelerates. In passing through the shock front, most of the infalling fluids kinetic energy is converted to thermal energy. The Post-Shock Accretion Column (PSAC), is therefore extremely hot $\sim 10^7$ K to 10^8 K and incredibly luminous, dominating the radiative output of the binary across a wide range of wavelengths. The response of the accretion column to perturbations, whether or not it will sustain oscillations or dampen them, depends sensitively on the cooling mechanisms at play within the post-shock region. If the radiative cooling is effective, the newly added hot gas will quickly shed its excess heat through photons and tend to contract, causing the initial perturbation to equilibrate. If, however, cooling is ineffective, the excess heat dumped in the post-shock region will continue driving expansion, contributing to the upward perturbation of the front. It can therefore be seen that under certain conditions, the PSAC is thermally unstable, giving rise to oscillations in the height of the shock front, the period of which is characterised by the cooling timescale of the post-shock gas as well as the mass accretion rate. Variance in the position of the front modulates the temperature and density of the shocked gas in the accretion column, consequently also modulating its luminosity and thus producing the observed QPO. The characteristics of any observed QPOs in the light curves of Polars when accompanied by the appropriate model, can therefore serve as a proxy for measuring the properties of the PSAC.

Although the model just described provides a plausible mechanism for generating QPOs, there are a number of discrepancies, most conspicuously, the absence of observed X-ray QPOs. An accretion column cooling predominantly through bremsstrahlung emission, is expected to produce X-rays. However, searches for X-ray QPOs in archival X-ray data from GINGA (Beardmore & Osborne, 1997) and XMM-Newton (Bonnet-Bidaud et al., 2015) have found no evidence for X-ray QPOs. The latter of these studies include a total of 24 Polars, including the 5 that, at the time of writing, were known to display optical QPOs.

Conclusions and Future work

Herein we have detailed the discovery of Quasi-Periodic Oscillations in the Polar J1928-50. The results presented here form part of a campaign at SAAO to search for- and characterise QPOs in Polar type mCVs in order to better understand these fascinating sources and the mechanisms that drive thier peculiar dynamic behaviour. Our observations cover the majority of known polars that are observable from the Southern hemisphere. Analysis of these data, totalling over 250 hours of high speed photometry, is currently ongoing, and will be presented in a forthcoming publication circa 2023.

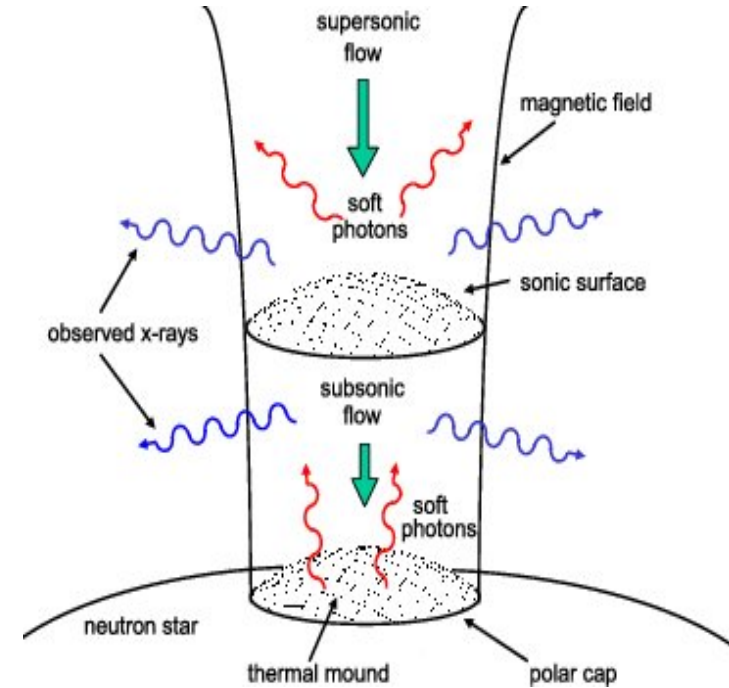


Figure 6: Schematic of the accretion column from Caballero & Wilms (2012).

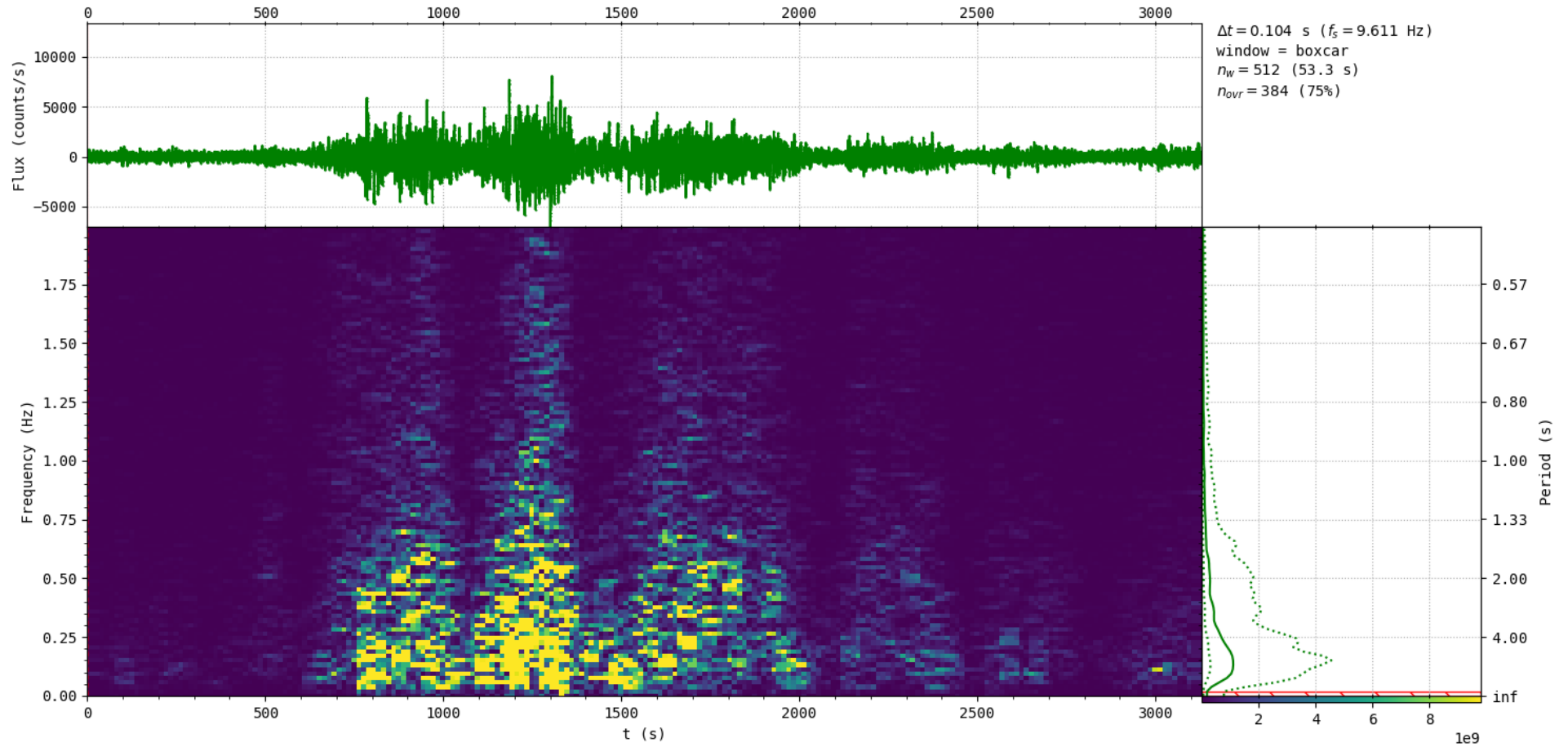


Figure 5: Time Frequency representation a.k.a. dynamic power spectrum of the SALTICAM light curve. **Upper panel:** A detrended version of the SALTICAM light curve presented in Figure 3. The low frequency variability has been removed by subtracting a smoothed version of the light curve averaged over a 100s moving window. **Central panel:** The dynamic power spectrum. Each column of the image represents the periodogram of a 512 point (53.3 s) section of the light curve. Successive windows overlap the previous by 75%. Increasing spectral power is represented linearly as an increase in pixel brightness, revealing the QPO as the central power excess above the white noise floor (dark pixels). **Right Panel:** The median periodogram along with upper and lower quartiles of the dynamic power spectrum. Power values corresponding to those in central panel are shown on the horizontal axis along with the colour bar.

References

- Maza, J., Ruiz, M. T., Gonzalez, L. E., and Wischnjewsky, M. (Mar. 1989). “Calan-Tololo Survey. I. Seyfert 1 Galaxies”. *ApJS* 69, 349. doi: 10.1086/191317 (cit. on p. 1).
- Beardmore, A. P. and Osborne, J. P. (Mar. 1997). “A GINGA hard X-ray search for 1-3s quasi-periodic oscillations in AM Herculis systems”. *MNRAS* 286.1, 77–80. doi: 10.1093/mnras/286.1.77 (cit. on p. 5).
- Tappert, C., Augusteijn, T., and Maza, J. (Oct. 2004). “Cataclysmic variables from the Calán-Tololo Survey - I. Photometric periods”. *MNRAS* 354.2, 321–331. doi: 10.1111/j.1365-2966.2004.08195.x (cit. on p. 1).
- Potter, S. B., Augusteijn, T., and Tappert, C. (Dec. 2005). “Photopolarimetric observations of the new eclipsing polar CTCVJ1928 - 5001”. *MNRAS* 364.2, 565–572. doi: 10.1111/j.1365-2966.2005.09569.x (cit. on pp. 1–3).
- Watson, C. L., Henden, A. A., and Price, A. (May 2006). “The International Variable Star Index (VSX)”. *Society for Astronomical Sciences Annual Symposium* 25, 47 (cit. on p. 2).
- Caballero, I. and Wilms, J. (June 2012). “X-ray pulsars: A review”. *Memorie della Societa Astronomica Italiana* 83 (cit. on p. 5).
- Scaringi, S., Körding, E., Uttley, P., Knigge, C., Groot, P. J., and Still, M. (Apr. 2012). “The universal nature of accretion-induced variability: the rms-flux relation in an accreting white dwarf”. *MNRAS* 421.4, 2854–2860. doi: 10.1111/j.1365-2966.2012.20512.x (cit. on p. 2).
- Drake, A. J., Gänsicke, B. T., Djorgovski, S. G., Wils, P., Mahabal, A. A., Graham, M. J., Yang, T. -, Williams, R., Catelan, M., Prieto, J. L., Donalek, C., Larson, S., and Christensen, E. (June 2014). “Cataclysmic variables from the Catalina Real-time Transient Survey”. *MNRAS* 441.2, 1186–1200. doi: 10.1093/mnras/stu639 (cit. on p. 2).
- Bonnet-Bidaud, J. M., Mouchet, M., Busschaert, C., Falize, E., and Michaut, C. (July 2015). “Quasi-periodic oscillations in accreting magnetic white dwarfs. I. Observational constraints in X-ray and optical”. *A&A* 579, A24. doi: 10.1051/0004-6361/201425482 (cit. on p. 5).
- Flesch, E. W. (Oct. 2016). “The Million Optical - Radio/X-ray Associations (MORX) Catalogue”. *PASA* 33, e052. doi: 10.1017/pasa.2016.44 (cit. on p. 2).
- Evans, P. A., Page, K. L., Osborne, J. P., Beardmore, A. P., Willingale, R., Burrows, D. N., Kennea, J. A., Perri, M., Capalbi, M., Tagliaferri, G., and Cenko, S. B. (Nov. 2019). “VizieR Online Data Catalog: 2SXPS Swift X-ray telescope point source catalogue (Evans+, 2020)”. *VizieR Online Data Catalog*, IX/58 (cit. on p. 2).
- Jayasinghe, T., Stanek, K. Z., Kochanek, C. S., Shappee, B. J., Holoiien, T. W. -, Thompson, T. A., Prieto, J. L., Dong, S., Pawlak, M., Pejcha, O., Shields, J. V., Pojmanski, G., Otero, S., Hurst, N., Britt, C. A., and Will, D. (May 2019). “The ASAS-SN catalogue of variable stars III: variables in the southern TESS continuous viewing zone”. *MNRAS* 485.1, 961–971. doi: 10.1093/mnras/stz444 (cit. on p. 2).